CHARACTERIZATION OF TRANSLOCON AND CARGO DYNAMICS DURING TAT TRANSPORT USING REAL-TIME KINETIC APPROACHES

A Thesis

by

NA WANG

Submitted to the Office of Graduate and Professional Studies of
Texas A&M University
in partial fulfillment of the requirements for the degree of

MASTER OF SCIENCE

Chair of Committee,	Siegfried Musser
Committee Members,	Sarah Bondos
	Raimund Ober
Head of Program,	Warren E. Zimmer

August 2017

Major Subject: Medical Sciences

ABSTRACT

Proteins must be translocated from ribosomes where they are synthesized to different cellular destinations where they perform their functions. Many different protein translocation systems carry out this activity like the human nuclear pore complex and the bacterial Sec and Tat machineries. In *Escherichia coli*, twin arginine translocation (Tat) system is used to transport fully folded proteins across the bacterial cytoplasmic membrane and the thylakoid membrane in plants without collapsing the ion gradients. A minimal Tat system consists of 3 integral membrane proteins: TatA, TatB and TatC. TatB and TatC form a receptor complex for the signal peptide of substrates. In the presence of a proton motive force and substrate, TatA is recruited to form the conducting channel allowing the mature domain of the substrate to migrate through it. After transport, TatA disassembles from the TatBC complex. Biochemical and biophysical work has provided information about the mechanism of Tat transport, however, the details of the mechanism are poorly understood. Therefore, we want to develop an in vitro transport assay at single vesicle level to characterize the sub-steps of Tat mechanism at the single vesicle level using total internal reflection fluorescence (TIRF) microscopy.

In vitro bulk experiments showed that the transport assay could be conducted at room temperature, which simplifies the assay under microscope by avoiding the temperature-control device. Additionally, ATP could replace NADH to generate PMF, which could maintain a longer membrane potential. 1.5% PVP could replace BSA to

avoid background fluorescence. Vesicles could be tethered on the coverslip surface by biotin-streptavidin linkage. Last, the pre-SufI with unnatural amino acid mutation in the signal peptide and cysteine mutation in the mature domain could not be labeled with Azide-Alexa647 and Alexa568 at the same time. In total, these results laid foundation for the in vitro transport assay at the single vesicle level.

DEDICATION

To my husband, my parents, my family and all the people who support me.

ACKNOWLEDGEMENTS

I would like to thank my advisor, Dr. Siegfried Musser, for his guidance, advice and patience. His overall enthusiasm for science and continued help was invaluable during my graduate studies.

I would like to thank my committee my committee members, Dr. Raimund Ober, Dr. Sarah Bondos, for their guidance and support throughout the course of this research.

I would like to thank all the current and former members of the Musser lab with whom I worked on a daily basis. Special thanks must be given to Dr. Shruthi Hamsanathan who trained me on the making inner membrane vesicles and in vitro transport assay and Dr. Guo Fu who helped me a lot on the operation of microscope.

Thanks also go to my friends and colleagues and the department faculty and staff for making my time at Texas A&M University a great experience.

Finally, thanks to my mother and father for their encouragement and to my husband for his patience and love.

CONTRIBUTORS AND FUNDING SOURCES

Contributors

This work was supervised by a thesis committee consisting of Professor Siegfried Musser as advisor and Professor Sarah Bondos of the Department Molecular Cellular Medicine and Professor Raimund Ober of Biomedical Engineering.

All work for the thesis was completed independently by the student.

Funding Sources

This work was made possible in part by the Welch Foundation under Grant Number BE-1541 to SMM and National Institutes of Health under Grant Number GM065534 to SMM.

Its contents are solely the responsibility of the authors and do not necessarily represent the official views of the Welch Foundation and National Institutes of Health.

NOMENCLATURE

$\Delta\psi$	electric field gradient
BSA	bovine serum albumin
FRET	fluorescence resonance energy transfer
IMVs	inner-membrane vesicles
NADH	beta-Nicotinamide adenine dinucleotide, reduced
PMF	proton motive force

TABLE OF CONTENTS

Page

LIST OF FIGURES

Page

CHAPTER I

INTRODUCTION AND LITERATURE REVIEW

SIGNIFICANCE

Biological and Medical Significance-Importance for Bacterial Growth and Human Health

Bacteria and archaea utilize two general export systems to translocate proteins across the cytoplasmic membrane to the periplasm. Sec-machinery mediated secretion is an essential pathway that provides for the transport of most proteins in an unfolded state and therefore is indispensable for bacterial growth. Tat system transports fully-folded and assembled proteins. The absence of a functional Tat system in bacteria often leads to growth defects and occasionally death. For example, the Tat system is essential for the growth of *Mycobacterium tuberculosis* (Mtb) (Saint-Joanis et al., 2006). Some Tat substrates are involved in the adaption of bacteria to a particular environment or play a role in virulence and the absence of a functional Tat system often leads to growth defects (Ochsner et al., 2002). For example, the enterohaemorrhagic *E. coli* serotype O157:H7 producing Shiga toxin is responsible for haemorrhagic colitis and haemolytic-uremic syndrome. A tatABC mutant (TatABC deleted) showed a fivefold decreased secretion of this toxin, an important virulence factor of *E. coli* O157:H7 and became less infectious (Pradel et al., 2003). Therefore, knowing the mechanism of the Tat system will help future studies on bacterial pathogenesis. Because the Tat pathway is conserved among

important bacterial pathogens and absent from mammalian cells, it could be a target for novel antimicrobial compounds against human and livestock pathogens.

Mechanistic Significance-Importance to This Field

To obtain insight into protein translocation mechanisms, the cargo is often trapped in the middle of the translocation process. The resultant structures are then analyzed by various techniques. However, up to now, no one in Tat field has successfully made Tat middle-state complexes. Several reasons hindered the process to understand the Tat mechanism, in particular, the later stages of transport. The fundamental problems attributes to the size, membranous nature, transience, low stability, and probable conformational and compositional heterogeneity of the translocation complex. Instead of trapping intermediates during transport, my goal is to examine the dynamics of various sub-steps of Tat translocation cycle in real-time at the single vesicle level. This study will clarify some sub-steps of Tat transport. In specific aim 1, we will develop an in vitro Tat transport assay at the single vesicle level. Ensemble fluorescence experiments are fundamentally limited by averaging and reaction synchrony issues. However, single molecule approaches eliminate these concerns and provide valuable information about the mechanism. In specific aim 2, we will characterize the kinetics of sub-steps of the Tat translocation process to distinguish between different models. The ultimate goal is to develop a detailed model of the sequence of events necessary for cargo transport.

BACKGROUND

General Secretion Systems

The Tat pathway functions in the bacterial plasma membrane and plant thylakoid membrane to transport proteins to the periplasm and thylakoid lumen, respectively (Barrett et al., 2007; Wickner and Schekman, 2005). The system is unusual among protein translocators because the substrates are translocated in a fully folded state. In parallel, the well-characterized Sec pathway translocates substrates in an unfolded state. The Sec and Tat pathways also differ in the energy usage during the translocation. The Sec machinery requires ATP hydrolysis and the proton motive force (PMF) while the Tat machinery instead depends solely on the PMF. Tat signal peptides are characterized by a RRXFLK consensus motif, which includes the twin-arginine (RR-motif) namesake ('Tat', for 'twin-arginine translocation')(Berks, 1996; Sargent et al., 1998). The Tat pathway plays key roles in many cellular processes, including photosynthetic and respiratory energy metabolism, nitrogen fixation, cell division, resistance to heavy metals and antimicrobial peptides, cell motility and virulence (Berks et al., 2003).

Tat Pathway Components

In *E. coli*, the minimal components required for Tat-dependent translocation consists of TatA, TatB and TatC (Sargent et al., 1998). TatA and TatB are homologous proteins and have similar core structures in which a short hydrophobic N-terminal helix is arranged approximately at right angles to an amphipathic helix (APH) and a highly charged, natively unstructured tail at the C-terminus. TatC, the largest and most conserved of the three Tat components, possesses 6 transmembrane helixes (TMHs),

which create a structure that resembles a cupped hand or glove. TatB proteins form constitutive, equimolar complexes with TatC, whereas TatA proteins oligomerize and increase their association with TatC in response to substrate binding to TatC to form the substrate mature domain transducing tunnel.

Tat Transport Mechanism

Unraveling the mechanisms of the Tat operation has been challenging because of the ephemeral nature of the translocase (Mori and Cline, 2002). However, the basic characteristics of the Tat translocation cycle have been experimentally determined using isolated pea thylakoids or *E. coli* inner-membrane vesicles (Fig 1). Firstly, Tat transport is initiated when the signal peptide of a substrate protein is recognized and bound by a multisubunit TatBC complex located in the membrane (Alami et al., 2003; Cline and Mori, 2001). Secondly, the binding of the signal peptide of the substrate to the TatBC receptor complex event triggers the PMF-dependent recruitment and oligomerization of TatA protomers from a pool in the membrane to form the active TatABC-containing translocation site. Thirdly, transport of the folded substrates across the lipid bilayer is assumed to be mediated by the assembled TatA oligomer. After completion of the transport, the substrate is released from the translocation site, the signal peptide is cleaved from the substrate mature domain by the signal peptidase (Luke et al., 2009; Yahr and Wickner, 2001), and the translocation site disassembles(Mori and Cline, 2002). How the Substrate Mature Domain Migrates Across the Bilayer is Unclear. Two general ‘pore models’ have been proposed. One states that TatA subunits line up to form substrate size-fitting channels (Gohlke et al., 2005; Sargent et al., 2006) based on the

observation that channel-like TatA structures of varying diameters are extracted from detergent treated non-transporting membranes(Gohlke et al., 2005). Such channels might be formed by 'charge zippers' from between the amphipathic helix and C-terminal densely charged region of TatA, and these insert into the membrane forming a hydrophilic TatA channel (Walther et al., 2013). The lipids remains within the pore and would diffuse away from the membrane, or, more likely, escape laterally into the membrane bilayer as the pore nears completion.

A popular alternative to the channel model proposes that Tat transport may work by weakening the membrane where the TatA molecules are concentrated (Walther et al., 2013). Substrate transport occur through transient bilayer rupture or once mechanical force has been exerted on the substrate to drive it through the weakened bilayer, in the meanwhile, the membrane remains intact and impermeable to ions, except at the moment of transport. The cell may tolerate the brief ion leakage that occurs during this transient opening of the bilayer. The lateral membrane pressure might cause the disordered phospholipids to pack around the substrates as it moves through the membrane. Evidence shows that Tat transport is strongly influenced by the membrane phospholipid composition, which is consistent with a mechanism involving protein-phospholipid interactions (Ma and Browse, 2006; Mikhaleva et al., 1999; Sikdar and Doerrler, 2010). Possible mechanisms include the interaction between the TatA APH and the cytoplasmic leaflet of the membrane (Bruser and Sanders, 2003; Greene et al., 2007) or the mismatch between the length of TatA TMH and the width of the bilayer (Rodriguez et al., 2013). MD simulations of the detergent-solubilized TatA oligomer structure into membrane

suggest that the mismatch mechanism might enable locally thinning the bilayer by about 80%, with the phospholipids in the thinned membrane showing high disorder (Rodriguez et al., 2013).

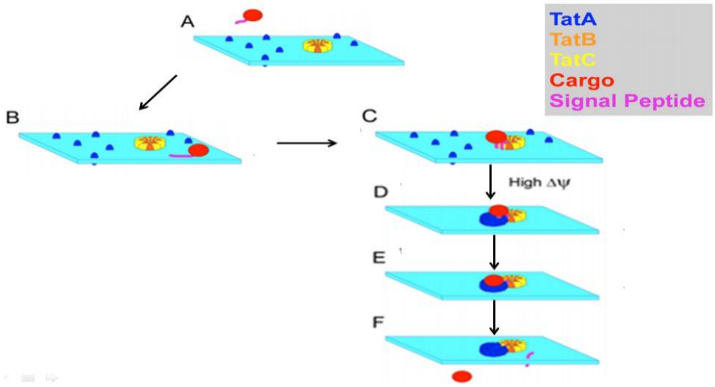

Fig 1. The cycle of *E.coli* Tat Transport in the channel model. TatB and TatC form the receptor complex, and TatA oligomerizes to form the translocation pore. The substrate binds to the membrane surface (B) in addition to the TatBC complex (C). (C-E) The transport processes. After transport, signal peptide cleavage occurs releasing the mature protein (F).

The Oligomerization State of TatBC Complex Remains Uncertain

Numerous studies have verified the stability and 1:1 stoichiometry of the TatBC heterodimer (Bolhuis et al., 2001; Maldonado et al., 2011; McDevitt et al., 2006; Orriss et al., 2007) but the oligomerization state of TatBC heterodimers remains controversial. Various models hypothesize that TatBC is fully functional as a dimer (Maldonado et al., 2011), trimer (Alcock et al., 2016) or a tetramer (Blummel et al., 2015). However, electron microscopy of detergent-solubilized TatBC reveals a ring-shaped structure

consistent with an octomer (Tarry et al., 2009). Other oligomers will be considered if necessary/warranted.

The Signal Peptide Binds the Membrane Bilayer Before Binding to the TatBC Complex or Not

Some studies report that a lipid-bound form of the precursor protein is not a requisite part of the translocation cycle, and, in fact, is a dead-end intermediate like the binding of at least some thylakoid substrates (Bruser and Sanders, 2003; Celedon and Cline, 2012). In contrast, other studies show that the precursor protein binds to membrane devoid of Tat proteins, suggesting that Tat precursors initially bind to membrane lipids and then diffuse to the TatBC complex (Bageshwar et al., 2009; Bruser and Sanders, 2003). Another independent study also indicates that the pre-SufI signal peptide binds to the phospholipid bilayer of IMVs, but does not penetrate the membrane surface in the absence of Tat proteins (Shruthi Hamsanathan, 2017).

Nevertheless, the mechanism for substrate transport remains very speculative, and demands more investigations. Detailed demonstration of substeps of the mechanism is still illusive. In order to picture the mechanism elaborately, an in vitro Tat transport assay at the single vesicle level will be developed to avoid the averaging and reaction synchrony issues (Parks et al., 2017).

CHAPTER II

EXPERIMENTAL DESIGN AND METHODS

QUESTIONS TO ADDRESS

To Develop an in Vitro Tat Transport Assay at the Single Vesicle Level

Conventional ensemble experiments have an inherent problem of averaging. In contrast, data from measurements in single molecule experiments offer a complete description of molecular structure, dynamics and function. In this way, possible heterogeneities can be readily identified. These heterogeneities can be either static, when various subpopulations of molecules remain unchanged over the observation time or dynamic, when there is some interconversion between molecular states during the observation time. The discovery of heterogeneities in biomolecular populations opened the way for answering important biological questions and also ignited the spark for raising new questions about how biological processes are taking place. Therefore, we would like to take the challenge to develop an in vitro Tat transport assay at the single vesicle level, aiming to provide more specific information about the Tat mechanism. The basic design of the real-time transport assay at the single IMV level in vitro will be as follows. IMVs will be immobilized on a coverslip, and total internal reflection fluorescence (TIRF) microscopy will be used to detect transport sub-steps in real time. A home-made flow cell will be used to add and remove reagents. Careful validation of the observations will be done to properly interpret the single molecule experiments.

Tether the IMVs on the Surface

To observe in vitro transport at the single vesicle level using TIRF microscopy, the vesicles need to be immobilized on a glass slide. The preparation of a surface that allows specific immobilization of molecules is one of the most critical steps in the single-molecule spectroscopy experiments.

Immobilization of IMVs on the Coverslip Surface

A specific immobilization of the vesicles is commonly ensured by biotin. After incubation of neutravidin or streptavidin (with its four biotin binding pockets), the biotinylated biomolecules can be easily attached to the surface via biotin-avidin linkage. The strong biotin-avidin interaction also ensures that the immobilized molecule does not detach prematurely and therefore can be monitored for hours. We utilized this method to tether vesicles on the coverslip.

The Effects of Biotinylation of IMVs on in Vitro Transport Efficiency

Biotin-avidin linkage is planned to be used to stabilize vesicles on the coverslip surface. 3-(N-maleimido-propinyl)-biocytin is the reagent used to biotinylate the IMV surface through random modification of cysteines in the membrane. Any modification of the membrane surface may affect substrate binding and transport across the membrane. Here we use TatC-cysteine free version of IMVs to prevent labeling of TatC with MPB. Result in preliminary data showed that the MPB modification of IMVs did not affect transport.

Temperature and Energy Source Effects on the in Vitro Transport

In general, in vitro transport assay is performed at 37℃, which is the physiological temperature of the *E. coli*. The transport efficiency was determined at room temperature. The result showed that the transport efficiency was high enough. This definitely simplified the microscope experiments by easier access to flow chamber by eliminating the need to install a temperature control device. Due to the scarcity of vesicles on the coverslip surface in the planned single molecule experiments and low cargo concentrations required to see single molecules, cargos are expected to infrequently bind to the IMVs. NADH may not be the ideal source to generate the PMF which depends on the dissolution of O_2 (Bageshwar and Musser, 2007). The alternative will be ATP. It generates a PMF through catalytic reversal of the F_0F_1 ATPase. With this approach, the $\Delta\psi$ is independent of the dissolved O_2 concentration and depends only on the ATP energy charge. Because ATP can be solubilized at higher concentrations than O2 and regenerated in situ, the $\Delta\psi$ gradient can be maintained for a longer period (Bageshwar and Musser, 2007). The result in the preliminary data showed that replacement of NADH by ATP wouldn't affect the transport efficiency.

Translocation into Coverslip-Adsorbed IMVs at the Single Vesicle Level.

Coverslip-adsorbed IMVs' functionality will be determined by the following two approaches. First, wild type IMVs (TatABC overexpressed IMVs) will be used. In this approach, IMVs will be immobilized on the coverslip surface. Protein translocation can be studied on the single vesicle level using precursor proteins labeled with a fluorescent fluorophore like pre-SufI. Pre-SufI with Alexa532 maleimide at the mature domain is

flowed through the flow cell. After incubating the IMVs and Alexa532 labeled pre-SufI for 30 min, I will wash away the unbound substrates. Then I will add NADH or ATP will to generate a PMF. The control is without adding either of the two reagents. The translocation process will be monitored and read as the accumulation of the Alexa532 labeled pre-SufI. Finally, 3-carboxy-PROXYL (3-CP) will be added to see whether the accumulation is resistant to it. 3-CP is a water-soluble, membrane-impermeant nitroxide (Yamada et al., 2004). If the accumulation is resistant to 3-CP, it indicates the substrates are transported inside the vesicle. If not, it means that the substrates just bind to the vesicle membrane. Similarly, urea/salt wash will be used to discriminate the binding or translocation. Expected results: Theoretically, without adding NADH or ATP, we see the association and dissociation of the substrates to the lipid membrane. It is not resistant to the 3-CP. With NADH or ATP, we expect to see the increase of the fluorescent intensity per vesicle will be significantly higher since several turnovers of protein translocation lead to more accumulation of pre-SufI inside the vesicles. The accumulation is resistant to the 3-CP. Similarly, in the binding scenario, the urea/salt wash will decrease the fluorescence in the IMV. However, if the substrates are transported into the vesicles, the wash will not change the fluorescence intensity.

Second, TatATatB^{cherry}TatC IMVs and Alexa488 labeled pre-SufI will be used to determine the functionality of coverslip-absorbed IMVs. M-cherry IMVs will be immobilized on the coverslip surface. The fluorescent M-cherry will be used to localize the vesicles. After incubating the IMVs and Alexa 488 labeled pre-SufI for 30 min, I will wash away the unbound substrates. Then, I will generate a PMF with NADH or ATP.

The control is without adding either of the two reagents. The translocation or binding can be verified by the co-localization of Alexa-488-pre-SufI and m-Cherry excited by 488 nm and 568 nm lasers individually. This accumulation will be tested by resistance to the 3-carboxy-PROXYL (3-CP) or urea/salt. Expected results: Theoretically, without adding NADH or ATP, we see the association and dissociation of the substrates to the lipid membrane. It is not resistant to the 3-CP. When NADH or ATP is added, the increase of the fluorescent intensity per vesicle will be significantly higher. We expect that several turnovers of protein translocation lead to more accumulation of pre-SufI inside the vesicles. The accumulation is resistant to the 3-CP. Similarly, in the binding scenario, the urea/salt wash will decrease the fluorescence in the IMV. However, if the substrates are transported into the vesicles, the wash will not change the fluorescence intensity.

<u>To Characterize the Kinetics of Sub-Steps of the Tat Translocation Process to Distinguish Between Different Models</u>

Determine the TatBC Oligomerization State.

TatATatB^{YFP}TatC IMVs will be generated. They will be tethered on the coverslip surface by the biotin-streptavidin linkage. Total internal reflection fluorescence (TIRF) microscopy will be used to photobleach the single vesicle. The fluorescence decrease data are recorded. As the control, the intensity of single YFP will be obtained from the fluorescence proteins. Analyze the fluorescence bleaching data of IMV with the single protein fluorescence intensity; I will know the copy number of TatB. Since the ratio of TatB and TatC is 1:1, the TatBC oligomerization state will be determined. Expected

results: Ideally, we could get the step-wise photobleaching at single vesicle (Fig 2). The observed distribution of photobleaching steps gives the likelihood of detecting a certain number of TatB or TatC within a single vesicle and we expect to see that the number of TatB or TatC in each single vesicle should follow a Poisson distribution with an average number of 1 or 2 based on the estimation.

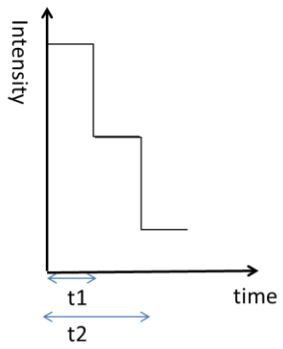

Fig 2 Example of step-wise photobleaching at the single vesicle level. With the time going, step number of photobleaching of TatB is counted. Note: the length for each step of intensity may be different due to the reason that two M-Cherry molecules are photobleached at the same time for example. t1 is the fluorescent time for one M-cherry and t2 is the fluorescent time for another M-cherry.

Use FRET to Demonstrate if Lipid-Bound Intermediate is Obligatory at Single Vesicle Level.

The layout of a typical objective-based TIRF single-molecule microscope is shown in Figure 3. This microscope is designed for excitation of fluorescence at three wavelengths. Fluorescence from the sample goes through the Opti Split III image splitter. This divides the image into three spectrally distinct components, which are imaged side

by side on an electron multiplication CCD (EMCCD) camera. To date, EMCCDs are the most suitable detectors for single molecule imaging because of their combination of high signal-to-noise with relatively fast readout speeds.

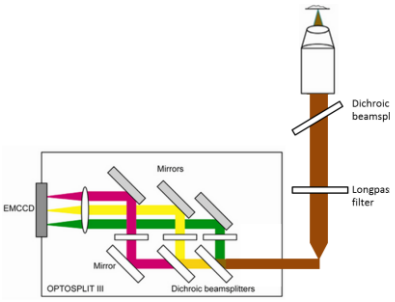

Figure 3 View of a microscope set up for 3-colour single molecule TIRF microscopy.

There is a divergence over whether the lipid-bound intermediate is a dead-end state. It is important to discriminate it since multiple aspects of our current transport model rely on a lipid-bound intermediate, at least for pre-SufI. We will directly determine the on-and off-rates for pre-SufI binding to the TatBC complex in single molecule experiments. A pre-SufI molecule that binds to an IMV is readily distinguished from a diffusing molecule by the sudden change in translational mobility. We will determine this via the labelled substrate-membrane FRET assay. TatATatBTatC-cherry IMVs (acceptor) and Alexa532 labeled-pre-SufI at position 29 or 96 (donor) (Whitaker et al., 2012) will be used. IMVs will be absorbed in the home-made chamber on the coverslip surface. Substrates and other reagents are flowed through the chamber. Total internal reflection fluorescence (TIRF) microscopy will be used to detect the binding events in real time. The increase and decrease in FRET will indicate association and

dissociation, respectively, from the TatBC complex (Fig 4). The two color images required to calculate FRET will be obtained by splitting the emission obtained via donor excitation onto two halves of an EMCCD camera. To prove the generality of the results, TatBC on-and off-rates will be determined for at least one additional precursor protein, e.g., spTorA-Alexa532-GFP.

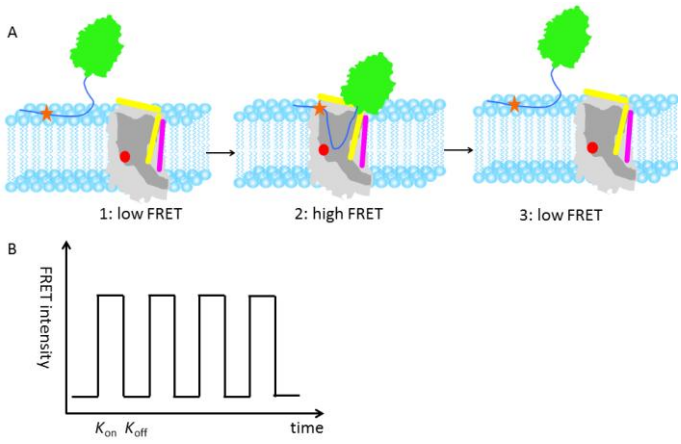

Fig 4 FRET to test the exchange between lipid binding and translocon binding. (A) At stage 1, the substrate binds to the membrane. The donor and acceptor (star and dot) are far away apart and low FRET signal is observed. At stage 2, the signal peptide is inserted into the TatBC complex, the distance between donor and acceptor is small and at this stage, we expect to see high FRET signal. Since substrate's binding to TatBC complex is a reversible process, at the stage 3, we see the dissociation between substrate and TatBC complex. Low FRET signal is seen. (B) The graph shows k_{on} and k_{off} indicating the association and dissociation of substrate and TatBC complex. Note: the time lenghts of k_{on} and k_{off} may be different.

FRET to Show When the Signal Peptide of Substrates is Cleaved

Fluorescence Labeling of Substrate Used in FRET-FRET requires both a donor dye and an acceptor dye. Because of the unsuccessful labelling of two fluorophores in one protein by the metal protection and labeling method using the cysteine-maleimide chemistry (Puljung and Zagotta, 2011), we would like to incorporate an unnatural amino acid into the protein and two independent labeling chemistries to get the dually labelled substrates. Unnatural amino acid (Uaa) incorporation by amber codon suppression using orthogonal aminoacyl-tRNA synthetase (aaRS)–amber suppressor tRNA ($tRNA_{CUA}$) pairs has flourished since 1998(Furter, 1998). The basic idea is to incorporate amber stop codon and cysteine by site-directed mutagenesis in the signal peptide of pre-SufI and mature domain, respectively. Label the protein with Azide-Alexa 647 and Alexa 568 at each site. We expect to get the dually labelled protein with the two fluorophores at a ratio 1:1. While the preliminary data indicated that after protein purification, the mature SufI dominated. To overcome this problem, we have two solutions. First, construct His-pre-SufI-11Uaa-58C mutant. Since the His tag is attached at the N-terminal of the signal peptide, only proteins with the signal peptide will be purified using Ni column. Second, Alexa 532 labeled His-TorA-F8C-Cherry will be used as an alternative substrate. Therefore, this protein has Alexa532 in the signal peptide and Cherry as the FRET pair. Recent progress in our lab indicated that His tag in the N terminal of signal peptide of TorA didn't affect the transport efficiency.

Labeling Efficiency and Specificity-Labeling efficiencies is evaluated by measuring the UV/vis absorbance spectra of the samples. SDS-PAGE of these samples

analyzed by fluorophore-imaging and Coomassie-staining indicates that labeling is very specific. The specificity of Alexa dye labeling was estimated by a comparison of the UV-vis absorbance spectra of the labeled protein with a cysteine-free and unnatural amino acid protein.

Effect of Dye Labeling on Transport Efficiency-In vitro transport assay will be done to determine whether the dye labeling will alter the function of pre-SufI across the membrane. When we do the labeling, the Azide-Alexa 647, Alexa 568 or Alexa 532 dyes will be attached to the protein surface, which will to some extent change the charge and hydrophobicity properties and further may affect the binding of substrate to the Tat translocon. Therefore, the in vitro transport efficiency of dual labeled protein will be tested.

Use FRET to Show When the Signal Peptide of Substrate is Cleaved-The basic design is pretty the same as the one in the aim2b but we will use WT vesicles and dually labeled pre-SufI as substrate instead. WT vesicles will be tethered on the coverslip surface and a flow chamber will be used to add or remove reagents. TIRF will be used to detect the FRET in real time. For this dually labeled pre-SufI protein, a decrease in donor (Alexa 568) will be observed in the absence of protease. An increase in donor (Alexa568) fluorescence will be observed in the presence of protease, consistent with loss of FRET, and under transport conditions, consistent with signal peptide cleavage after transport (Fig 5).

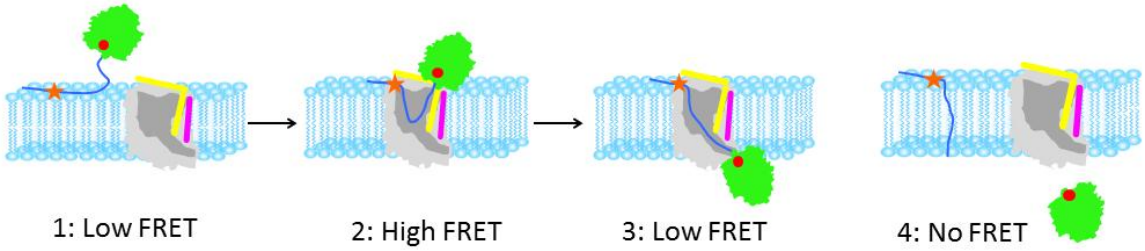

Fig 5 FRET to test the signal peptide cleavage. Here I use dual labeled pre-SufI to illustrate how to use FRET to test the signal peptide cleavage. In stage 1, the substrate pre-SufI binds to membrane and may have a configuration to give a low FRET signal. In state 2, the signal peptide inserts into the TatBC complex to make the distance between donor and acceptor shorter. A strong FRET signal could be observed. In state 3, the mature domain migrates to the cytoplasm side to make the distance between donor and acceptor larger. A weak signal may be seen. 4, after the cleavage, the distance between donor and acceptor exceeds 10nm and therefore leads to loss of FRET signal.

CHAPTER III

CONCLUSIONS

IN VITRO TRANSPORT AT ROOM TEMPERATURE

The basics of in vitro transport assay are as follows. Inverted inner membranes vesicles (IMVs) are obtained from E.coli cells overexpressing TatABC by French Press treatment and sucrose gradient purification. The precursors (cargos) overexpressed and purified from E.coli are transported into the IMV lumen at 37℃ in the presence of a PMF. A PMF is generated by NADH (a respiratory substrate) or ATP (which generates a PMF by reversal of the ATP synthase). Transport is confirmed by protease treatment (which digests protein that remains outside the IMVs) and the presence of a lower molecular weight band due to signal peptide cleavage (resulting in mature protein) on an SDS-PAGE gel. The cargo is visualized on gels by Western blotting or direct in-gel fluorescence (for dye-labeled proteins). Our transport efficiencies are typically high (~ 20-50%, depending on conditions). For comparison, most protein translocation studies report translocation efficiencies< 20% (Fig 6A).

Our lab developed in vitro transport assay with high efficiency (~20-50%). In order to simplify in vitro transport assay under microscope by easy access to the flow chamber, we tested whether transport was efficient at room temperatures. The assay was carried out following standard protocol under 37℃, 22℃ and 30℃ using the natural substrate pre-SufI-IAC as the model cargo. Result showed that the transport efficiency

under room temperature (22℃) is 83.1% comparable to the efficiency under 37℃ (Fig 6B).

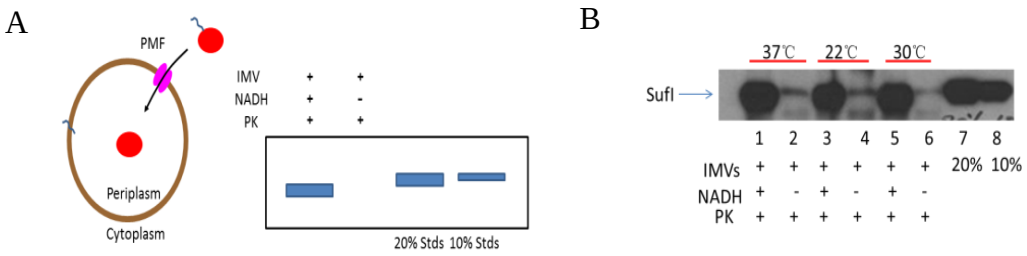

Fig 6. In vitro transport at room temperature test. (A) Schematic of In Vitro Tat Transport Assay. For IMVs, the 'cytoplasm' is outside, and Tat cargos (pre-proteins) are transported into the IMV lumen. The signal peptide (blue) is separated from the mature domain (red) by signal peptidase after transport. Transport is verified using SDS-PAGE by the presence of a protease-protected mature protein. (B) Effect of temperature on in vitro Tat transport assays. The gel shows anti-SufI immunoblot of transport of pre-sufI into IMVs overexpressing TatABC. Transport requires NADH to generate the necessary PMF. In the anti-SufI immunoblot, known amounts of pre-SufI (lanes 7-8), marked as a percentage of precursor protein added to the transport reactions, allowed quantification of the transport efficiency. Samples were treated by protease K for 42 min at 37℃ (lane 1-2), 22℃(lane 3-4) and 30℃(land 5-6) respectively. Efficient transport occurred under different temperatures. [pre-SufI]=90nM; [IMV]=5(A280).

ENERGY SOURCE AND BLOCKING AGENT

Then, I wanted to test whether NADH could be replaced by ATP. NADH is normally used to generate a PMF. ATP was used since we wanted the PMF can be

maintained for a longer period. ATP generates a PMF through catalytic reversal of the F_0F_1 ATPase, which is independent of the dissolved O_2 concentration and depends only on the ATP energy charge. ATP can be solubilized at higher concentrations than O_2 and regenerated in situ, the electric field gradient can be maintained for a longer period (Bageshwar and Musser, 2007). Result showed that ATP didn't affect the in vitro transport efficiency.

BSA is used to block the Eppendorf tube in the in vitro transport assay. However, BSA may give background fluorescence under microscope. 1.5% PVP was the reagent to replace it. PVP didn't affect the in vitro transport efficiency (Fig7).

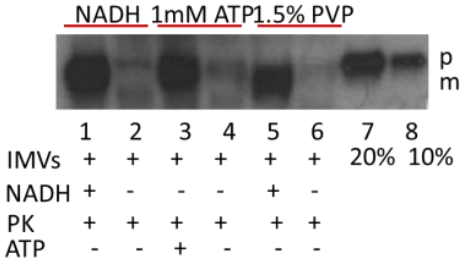

Fig 7. Effects of ATP and 1.5% PVP on the in vitro transport assays. In this anti-SufI immunoblot of transport of pre-sufI into IMVs overexpressing TatABC, lanes 7-8 shows the percentage of precursor protein added to the transport reactions, allowing quantification of the transport efficiency. Compared to 4 mM NADH to generate the PMF (lane 1-2), 1 mM ATP does not affect the transport efficiency (lanes 3-4). 1.5% PVP instead of 10 mg/ml BSA to coat the Eppendorf tube didn't affect the transport efficiency (lanes 5-6). [pre-SufI]=90nM; [IMV]=5(A280).

BIOTINLATION OF IMVs

Inverted membrane vesicles (IMVs) from *E. coli* were isolated and labeled with Alexa568. Alexa568 was used because it also has the maleimide-reacting group. MPB contains two groups: maleimide and biotin. Maleimide was used to label the exposed cysteines in the membrane to generate the biotinylated IMVs. If IMVs can be labeled with Alexa568, it meant that it can be labeled with MPB. At the Alexa568 concentration of 2uM, we saw observable labeling of IMVs. Increasing the concentration, more labeling was seen (Fig 8A). We next tested the transport efficiency of pre-SufI into MPB labeled IMVs since biotin modification on the membrane may alter the efficiency. Alexa568-pre-SufI was used as the substrate. We found that this modification didn't affect the transport efficiency (Fig 8B). In order to observe in vitro transport at the single vesicle level on the coverslip under a microscope, we need to tether the vesicles on the coverslip since transport events can't be observed when the IMVs are moving in the solution. To achieve this, 50uL 0.2mg/mL streptavidin in water was loaded on the surface of coverslip, allowed to sit for at least 60min, then washed away with 300uL H2O. Biotinylated IMVs at 0.1OD were applied to the chamber. Biotin-streptavidin linkage was expected to form and IMVs were tethered on the surface. The IMVs were visualized by Nile-red, a dye to stain the neutral lipid in the membrane. Results showed that vesicles were only stabilized on streptavidin coated surface (Fig 8C) .

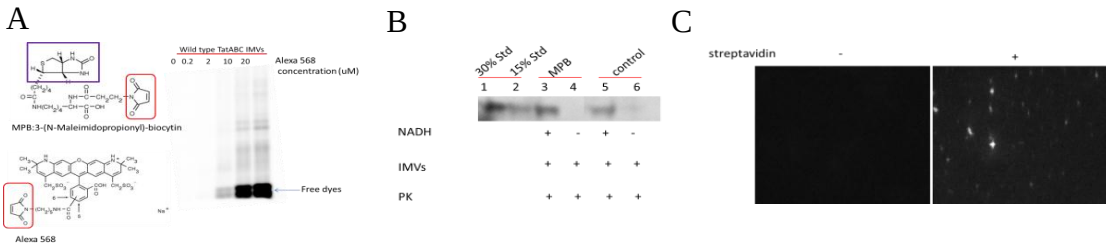

Fig 8. Effect of MPB on in vitro transport efficiency of Alexa568-pre-SufI and tethering of IMVs on the coverslip surface.

MPB (3-(N-Maleimidopropionyl)-biocytin) and Alexa568 have the same maleimide-reacting group. Alexa568 was used to show that random proteins with cysteines in the membrane of vesicles can be labeled with maleimide. The gel in this figure is visualized by fluorescence emission upon laser 555 excitation. At 2uM Alexa568, observable labeling of IMVs was seen. Increasing concentration of Alexa568 leaded to stronger labeling of IMVs. Red and purple boxes show maleimide group and biocytin group respectively. (B) The gel in this figure is visualized by fluorescence emission upon laser 555 excitation. Lanes 1-2 shows the percentage of precursor protein added to the transport reactions, allowing quantification of the transport efficiency. IMVs without MPB labeling were taken as control (lane5-6). Compared to the control, IMVs with MPB labeling didn't show decreased in vitro transport efficiency of Alexa568-pre-SufI. (C) Tethering of IMVs on the coverslip surface. Coverslip surface wasn't coated with streptavidin. Biotin-labeled IMVs weren't tethered on the coverslip surface (Left). Note: the fluorescence dots in the image didn't indicate that the IMVs were tethered on the coverslip surface while it is one image from a moive. In contrast, coverslip was coated with 0.2mg/mL streptavidin. Biotin-labeled IMVs were tethered on the coverslip surface (Right).

DOUBLE LABELING OF PRE-SUFI

In order to get the substrates for FRET with donor and acceptor at the same protein, the 11A in the signal peptide and 58S were mutated to unnatural amino acid and cysteine through site directed mutagenesis, respectively. The A11Uaa (unnatural amino acid) was labeled with Azide-Alexa647 by the copper (I)-catalyzed alkyne-azide cycloaddition (CuAAC) reaction. Copper(I)-Catalyzed Azide-Alkyne Cycloaddition (CuAAC) forms a 1,4-disubstituted-1,2,3-triazole by an azide and a terminal alkyne when in the presence of a copper(I) catalyst and copper(I)-binding ligand. The S58C was labeled with Alexa568 through maleimide-thiol reaction. At the very beginning, we tested whether the two dyes could label the pre-SufI at the same time. If this occurred, time would be saved. Therefore, the pre-SufI was reduced by copper and then incubated with both dyes. Results showed that copper reduced the Alexa568 maleimide labeling in the mature domain of pre-SufI and therefore we couldn't label pre-SufI with the two dyes at the same time (Fig 9A). Noticeably, the Azide-Alexa647 band always has a higher molecule weight than the Alexa568 band but ideally the two bands should overlap together. Since Alexa647 only labels protein with signal peptide, we suspected that the purified protein was predominantly mature SufI. This likely occurred for 2 reasons. Firstly, unnatural amino acids typically lower the yield of proteins since they have to compete with the release factor. Secondly, the signal peptide of pre-SufI was cut off by cytoplasmic peptidase, a problem which is particularly acute when the expression level was low. In order to confirm our guess, we run two single cysteine mutants of pre-SufI as controls in parallel with pre-SufI-58C-11-Uaa. The results showed that for the

controls, although there were some mature forms of SufI, the pre-SufI dominated. While for the pre-SufI-58C-11-Uaa, we barely saw the precursor form of pre-SufI (Fig 9B).

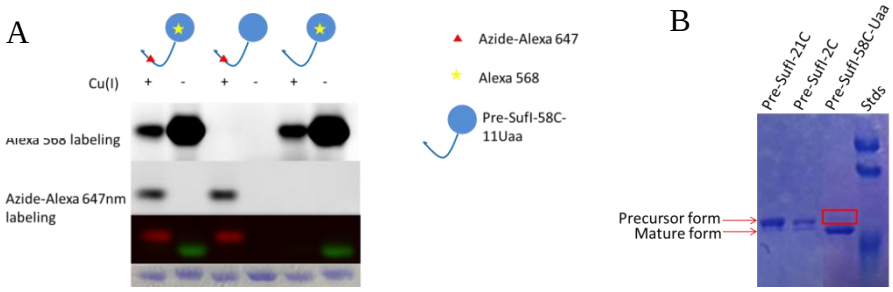

Fig 9. Labeling of pre-SufI with Azide-Alexa647 and Alexa568. (A) The gel in this figure is visualized by fluorescence emission upon laser 555 and 647 excitation. Coomassie blot showed equal loading amount. Pre-SufI is labeled with Azide-Alexa647 in the signal peptide and Alexa568 in the mature domain lane1-2). Only in the presence of copper (+), pre-SufI was labeled by Azide-Alexa647. As to Alexa568, copper decreased pre-SufI labeling (lane 1 and 2). Lane 3 and 4 showed pre-SufI was labeled with Azide-Alexa 647. It indicated that the Azide-Alexa647 is only labeled in the presence of copper. Lane 5 and lane 6 showed that pre-SufI was labeled with Alexa 568. It indicated that copper decreased Alexa 568 labeling. However, from the pseudo color overlap, Azide-Alexa647 was higher than Alexa568. (B) The right gel was visualized by Coomassie staining. It explained why the Azide-Alexa647 band was higher than Alexa568. Two single cysteine mutants pre-SufI-21C and pre-SufI-2C (left two lanes) ran parallel with the mutant contained cysteine and unnatural amino acid pre-SufI-58C-Uaa (3rd lane from left to right). After purification, the mature form of pre-SufI-58C-Uaa occupied mostly. This well explained Azide-Alexa647 band was higher than Alexa568.

REFERENCES

Alami, M., Luke, I., Deitermann, S., Eisner, G., Koch, H.G., Brunner, J., and Muller, M. (2003). Differential interactions between a twin-arginine signal peptide and its translocase in *Escherichia coli*. Mol Cell *12*, 937-946.

Alcock, F., Stansfeld, P.J., Basit, H., Habersetzer, J., Baker, M.A.B., Palmer, T., Wallace, M.I., and Berks, B.C. (2016). Assembling the Tat protein translocase. eLife *5*, e20718.

Bageshwar, U.K., and Musser, S.M. (2007). Two electrical potential-dependent steps are required for transport by the Escherichia coli Tat machinery. J Cell Biol *179*, 87-99.

Bageshwar, U.K., Whitaker, N., Liang, F.C., and Musser, S.M. (2009). Interconvertibility of lipid- and translocon-bound forms of the bacterial Tat precursor pre-SufI. Mol Microbiol *74*, 209-226.

Barrett, C.M., Freudl, R., and Robinson, C. (2007). Twin arginine translocation (Tat)-dependent export in the apparent absence of TatABC or TatA complexes using modified Escherichia coli TatA subunits that substitute for TatB. J Biol Chem *282*, 36206-36213.

Berks, B.C. (1996). A common export pathway for proteins binding complex redox cofactors? Mol Microbiol *22*, 393-404.

Berks, B.C., Palmer, T., and Sargent, F. (2003). The Tat protein translocation pahway and its role in microbial physiology. Adv Microbiol Physiol *47*, 187-254.

Blummel, A.S., Haag, L.A., Eimer, E., Muller, M., and Frobel, J. (2015). Initial assembly steps of a translocase for folded proteins. Nat Commun *6*, 7234.

Bolhuis, A., Mathers, J.E., Thomas, J.D., Barrett, C.M., and Robinson, C. (2001). TatB

and TatC form a functional and structural unit of the twin-arginine translocase from Escherichia coli. J Biol Chem *276*, 20213-20219.

Bruser, T., and Sanders, C. (2003). An alternative model of the twin arginine translocation system. Microbiol Res *158*, 7-17.

Celedon, J.M., and Cline, K. (2012). Stoichiometry for binding and transport by the twin arginine translocation system. J Cell Biol *197*, 523-534.

Cline, K., and Mori, H. (2001). Thylakoid ΔpH-dependent precursor proteins bind to a cpTatC-Hcf106 complex before Tha4-dependent transport. J Cell Biol *154*, 719-729.

Furter, R. (1998). Expansion of the genetic code: site-directed p-fluoro-phenylalanine incorporation in Escherichia coli. Protein Sci *7*, 419-426.

Gohlke, U., Pullan, L., McDevitt, C.A., Porcelli, I., de Leeuw, E., Palmer, T., Saibil, H.R., and Berks, B.C. (2005). The TatA component of the twin-arginine protein transport system forms channel complexes of variable diameter. Proc Natl Acad Sci U S A *102*, 10482-10486.

Greene, N.P., Porcelli, I., Buchanan, G., Hicks, M.G., Schermann, S.M., Palmer, T., and Berks, B.C. (2007). Cysteine scanning mutagenesis and disulfide mapping studies of the TatA component of the bacterial twin arginine translocase. J Biol Chem *282*, 23937-23945.

Luke, I., Handford, J.I., Palmer, T., and Sargent, F. (2009). Proteolytic processing of *Escherichia coli* twin-arginine signal peptides by LepB. Arch Microbiol *191*, 919-925.

Ma, X., and Browse, J. (2006). Altered rates of protein transport in Arabidopsis mutants deficient in chloroplast membrane unsaturation. Phytochemistry *67*, 1629-1636.

Maldonado, B., Buchanan, G., Müller, M., Berks, B.C., and Palmer, T. (2011). Genetic evidence for a TatC dimer at the core of the *Escherichia coli* twin arginine (Tat) protein translocase. J Mol Microbiol Biotechnol *20*, 168-175.

McDevitt, C.A., Buchanan, G., Sargent, F., Palmer, T., and Berks, B.C. (2006). Subunit composition and in vivo substrate-binding characteristics of *Escherichia coli* Tat protein complexes expessed at native levels. FEBS J *273*, 5656-5668.

Mikhaleva, N.I., Santini, C.L., Giordano, G., Nesmeyanova, M.A., and Wu, L.F. (1999). Requirement for phospholipids of the translocation of the trimethylamine N-oxide reductase through the Tat pathway in Escherichia coli. FEBS Lett *463*, 331-335.

Mori, H., and Cline, K. (2002). A twin arginine signal peptide and the pH gradient trigger reversible assembly of the thylakoid ΔpH/Tat translocase. J Cell Biol *157*, 205-210.

Ochsner, U.A., Snyder, A., Vasil, A.I., and Vasil, M.L. (2002). Effects of the twin-arginine translocase on secretion of virulence factors, stress response, and pathogenesis. Proc Natl Acad Sci U S A *99*, 8312-8317.

Orriss, G.L., Tarry, M.J., Ize, B., Sargent, F., Lea, S.M., Palmer, T., and Berks, B.C. (2007). TatBC, TatB, and TatC form structurally autonomous units within the twin arginine protein transport system of *Escherichia coli*. FEBS Lett *581*, 4091-4097.

Parks, J.W., Kappel, K., Das, R., and Stone, M.D. (2017). Single-molecule FRET-Rosetta reveals RNA structural rearrangements during human telomerase catalysis. RNA *23*, 175-188.

Pradel, N., Ye, C., Livrelli, V., Xu, J., Joly, B., and Wu, L.F. (2003). Contribution of the

twin arginine translocation system to the virulence of enterohemorrhagic Escherichia coli O157:H7. Infect Immun *71*, 4908-4916.

Puljung, M.C., and Zagotta, W.N. (2011). Labeling of specific cysteines in proteins using reversible metal protection. Biophys J *100*, 2513-2521.

Rodriguez, F., Rouse, S.L., Tait, C.E., Harmer, J., De Riso, A., Timmel, C.R., Sansom, M.S., Berks, B.C., and Schnell, J.R. (2013). Structural model for the protein-translocating element of the twin-arginine transport system. Proc Natl Acad Sci U S A *110*, E1092-1101.

Saint-Joanis, B., Demangel, C., Jackson, M., Brodin, P., Marsollier, L., Boshoff, H., and Cole, S.T. (2006). Inactivation of Rv2525c, a substrate of the twin arginine translocation (Tat) system of Mycobacterium tuberculosis, increases beta-lactam susceptibility and virulence. J Bacteriol *188*, 6669-6679.

Sargent, F., Berks, B.C., and Palmer, T. (2006). Pathfinders and trailblazers: a prokaryotic targeting system for transport of folded proteins. FEMS Microbiol Lett *254*, 198-207.

Sargent, F., Bogsch, E.G., Stanley, N.R., Wexler, M., Robinson, C., Berks, B.C., and Palmer, T. (1998). Overlapping functions of components of a bacterial Sec-independent protein export pathway. EMBO J *17*, 3640-3650.

Sikdar, R., and Doerrler, W.T. (2010). Inefficient Tat-dependent export of periplasmic amidases in an Escherichia coli strain with mutations in two DedA family genes. J Bacteriol *192*, 807-818.

Tarry, M.J., Schäfer, E., Chen, S., Buchanan, G., Greene, N.P., Lea, S.M., Palmer, T.,

Saibil, H.R., and Berks, B.C. (2009). Structural analysis of substrate binding by the TatBC component of the twin-arginine protein transport system. Proc Natl Acad Sci U S A *106*, 13284-13289.

Walther, T.H., Gottselig, C., Grage, S.L., Wolf, M., Vargiu, A.V., Klein, M.J., Vollmer, S., Prock, S., Hartmann, M., Afonin, S.*, et al.* (2013). Folding and self-assembly of the TatA translocation pore based on a charge zipper mechanism. Cell *152*, 316-326.

Whitaker, N., Bageshwar, U.K., and Musser, S.M. (2012). Kinetics of precursor interactions with the bacterial Tat translocase detected by real-time FRET. J Biol Chem *287*, 11252-11260.

Wickner, W., and Schekman, R. (2005). Protein translocation across biological membranes. Science *310*, 1452-1456.

Yahr, T.L., and Wickner, W.T. (2001). Functional reconstitution of bacterial Tat translocation *in vitro*. EMBO J *20*, 2472-2479.

Yamada, K., Inoue, D., Matsumoto, S., and Utsumi, H. (2004). In vivo measurement of redox status in streptozotocin-induced diabetic rat using targeted nitroxyl probes. Antioxid Redox Signal *6*, 605-611.